JOURNAL OF GEOPHYSICAL RESEARCH, VOL. 89, NO. C3, PAGES 3473–3486, MAY 20, 1984

Seasonal Variability of Alongshore Geostrophic Velocity Off Central California

DUDLEY B. CHELTON

College of Oceanography, Oregon State University

Seasonal variability of alongshore geostrophic velocity relative to 500 dbar is examined from 23 years of hydrographic data along two sections off central California (one off Point Sur and the other off Point Conception). The seasonal cycles are determined by least square fits of the gappy data records to harmonics with annual and semiannual periods. Attention is focused on variability over the outer continental slope. Geostrophic flow in the upper 100 m along both sections is coherent and predominantly annual with equatorward flow from February to September and poleward flow from October to January. The flow deeper than 100 m is distinctly different along the two sections. The nearshore deep flow is predominantly semiannual off Point Conception (notably different from surface flow) and poleward all year with maxima in December and June. This semiannual variability at depth is a prevalent feature of the California Current system. The nearshore deep flow off Point Sur is unusual in that it is predominantly annual with maximum poleward flow in December and weak equatorward flow from March to May. The seasonal variations over the continental slope compare favorably with existing models of eastern boundary current systems in two respects: (1) The surface flow leads the predominantly annual wind forcing in this region by about one month; and (2) the deep poleward counterflow is coherent with the local poleward barotropic pressure gradient at both locations, with a phase lag of approximately 2 months. However, contrary to the results of existing dynamical models, the semiannual poleward pressure gradient and undercurrent off Point Conception appear to be unrelated to the wind forcing, which is predominantly annual in this region. These semiannual variations are highly coupled to the semiannual flow throughout the water column inside the Southern California Bight, suggesting that they may be topographically generated.

1. INTRODUCTION

Dynamical modeling of eastern boundary current systems has received a great deal of attention in recent years. These studies have been largely motivated by the rather intriguing and complex structure of the flow observed in these regions. The features apparently common to all eastern boundary currents consist of a broad surface equatorward flow with a deep subsurface poleward undercurrent over the continental slope. Models have now advanced to a stage where they have begun to examine fully three-dimensional time-dependent variations in eastern boundary current systems. Numerous observations have documented the presence of equatorward surface currents and poleward undercurrents, but relatively few studies have described variability of the currents over time scales longer than a few weeks. Observations of the time-dependent flow are now an essential element for directing future modeling efforts.

Although not ideally suited to the study of velocity, hydrographic data from a long-term survey of the southern California Current can provide useful information on the spatial and temporal structure of the flow in the region from San Francisco to the southern tip of Baja California. These observations were initiated in 1949 as part of an ecological study of the California Current System by the California Cooperative Oceanic Fisheries Investigations (CalCOFI). The original purpose was to evaluate the effects of environmental changes on the declining sardine stock. After the collapse of the California sardine fishery in 1953, the hydrographic surveys continued with emphasis shifted to study of the underlying principles governing behavior, availability and total abundance of other pelagic fish stocks in the California Current. CalCOFI surveys have continued through 1981, resulting in possibly the most extensive hydrographic data set in existence anywhere in the world oceans.

An important aspect of the CalCOFI hydrographic survey for the analysis presented here is that a geographically fixed sampling grid was established in 1950 and maintained throughout the remainder of the program. Thus, time series of water density can be constructed for each grid point at selected standard depths throughout the water column. Seasonal variations can then be determined from the time series by using the method described in the appendix. In this study, these seasonal variations of density are used to compute at each standard depth the seasonal alongshore component of geostrophic velocity relative to a reference level of 500 dbar. For simplicity, these velocity shears will be referred to throughout this paper as geostrophic velocity with the understanding that they are actually relative geostrophic velocities; they correspond to true geostrophic velocity only if the 500 dbar surface is a level surface.

One of the characteristics of eastern boundary currents of particular interest in this study is the poleward undercurrent generally found at depths greater than 100 m. The relation between undercurrents over the shelf and continental slope is not well known. The region studied here is limited to water deeper than 500 m. Particular attention will be focused on the outer continental slope region which we will define to be that part of the continental slope in water deeper than 500 m. The coupling between shelf and slope undercurrents is better investigated with direct current meter observations or hydrographic data with greater spatial resolution than is presently available.

Because of the complex bottom topography south of Point Conception, the present study is restricted to the northern portion of the CalCOFI sampling domain, ranging from Monterey to Point Conception. The seasonal relative geostrophic velocities are described in section 5. The purpose is to establish from the CalCOFI data some diagnostic features of the time-varying flow field. A discussion of the results in light of

Paper number 4C0135.
0148-0227/84/004C-0135$05.00

existing dynamical frameworks is given in section 6. Before presentation of these new results, a review of observational and theoretical studies of the California Current System will be given in sections 2 and 3.

2. OBSERVATIONAL BACKGROUND

On the basis of early data collected off the coasts of California and Peru, *Sverdrup et al.* [1942] speculated that the eastern boundary currents of all subtropical gyres share a number of common features. A more recent review by *Wooster and Reid* [1963] showed that, with the exception of the West Australian Current, all eastern boundary currents are, indeed, similar. The flow can be generally characterized by a slow, predominantly equatorward movement of cold fresh water with very little motion below 1000 m. There is no sharp western edge but most of the net equatorward transport occurs within 1000 km of the coast. The flow tends to be highly variable in both space and time. This is particularly true over the continental shelf where fluctuating "events" of poleward and equatorward jetlike surface currents are superimposed on a slowly varying mean flow. The flow in regions farther offshore is also highly variable with the presence of numerous eddies and meanders.

The most conspicuous feature of eastern boundary currents is a subsurface poleward flow sometimes found over the shelf and nearly always observed over the continental slope at depths below 100 m. This poleward flow occasionally extends to the surface and is counter to the generally equatorward winds in these regions. Early studies identified eastern boundary undercurrents from water mass characteristics. Off the west coasts of North and South America, they are recognized as a subsurface salinity maximum with high temperature and salinity and low oxygen content characteristic of near-surface equatorial waters.

This review is limited to a summary of observational studies in the California Current System, which is the most extensively studied of all eastern boundary current regions. The earliest systematic observational studies were conducted off southern California in spring and summer of 1937 [*Sverdrup and Fleming*, 1941; *Sverdrup et al.*, 1942]. An undercurrent below 200 m was noted, and it was suggested that, in the absence of prevailing equatorward winds, the subsurface poleward flow would extend to the surface. They argued that the strong spring and summer winds drive an equatorwarad surface jet which overrides the poleward counterflow in the upper 200 m.

In 1949, under the direction of H. Sverdrup, a long-term hydrographic survey of the California Current System was initiated. As discussed in section 1, these hydrographic measurements were part of a much larger physical, chemical, and biological program by CalCOFI to study the ecosystem of the southern California Current. *Reid et al.* [1958] synthesized the first few years of CalCOFI hydrographic data and summarized some aspects of seasonal variability from northern California to the southern tip of Baja California. There is an annual progression of equatorward winds from south to north such that the winds are maximum in spring off Baja and in summer off Oregon. (Note, however, that upwelling off Oregon is most intense in spring, preceding the maximum local equatorward wind stress by several months (see works by *Huyer et al.* [1975], *Hickey* [1979], and *Hickey and Pola* [1983]).) During these periods of strong equatorward winds, the surface flow is equatorward everywhere along the west coast except within the Southern California Bight region from Point Conception to northern Baja where there is a quasi-permanent cyclonic eddy with poleward flow near the coast. Direct measurements by drift bottles and GEK current meters indicate that this poleward surface flow extends north of Point Conception only in late fall and early winter when the equatorward winds are weakest [*Reid et al.*, 1958; *Reid and Schwartzlose*, 1962]. During this time the poleward flow in the Southern California Bight appears to be part of a much larger scale nearshore surface countercurrent which extends from southern Baja to Oregon and Washington (called the Davidson Current).

At depths below 200 m, *Reid et al.* [1958] showed from dynamic topography of the 200 dbar surface that there is poleward flow throughout most of the year from southern Baja to at least as far north as Cape Mendocino in northern California. This geostrophic flow has been subsequently verified from direct measurements by drogues [*Reid*, 1962, 1963] and current meters [*Wooster and Jones*, 1970].

A more comprehensive summary of seasonal variability has been given by *Wyllie* [1966] in an atlas based on data acquired during the first 16 years of the CalCOFI program (1950–1965). Maps of long-term average dynamic topography of the 0 and 200 dbar surfaces relative to 500 dbar are presented for each calendar month. (Weaknesses of this method of determining seasonal variability are discussed in the appendix.) The features described by *Reid et al.* [1958] based on only the first few years of CalCOFI data are more clearly defined in the Wyllie maps constructed from the much larger data base. A more recent CalCOFI atlas by *Lynn et al.* [1982] summarizes the seasonal hydrographic variability from 1950 to 1978, using a similar long-term averaging technique.

An exhaustive review and synthesis of progress in studies of the California Current System has been given by *Hickey* [1979]. Geostrophic velocities relative to 500 dbar were computed from the dynamic height data of *Wyllie* [1966]. Of particular interest to the present study is Hickey's discussion of the undercurrent over the outer continental slope. From nearshore geostrophic velocities at 200 dbar relative to 500 dbar at Cape Mendocino and Point Conception, there is some indication that the poleward flow of the undercurrent has two seasonal maxima, one in summer or early fall and another in winter. Hickey suggests that this semiannual variability reflects a response to a complex combination of forcing mechanisms: A nearshore poleward mean flow is driven by the nearshore mean positive wind stress curl. Superimposed on this mean flow are a winter maximum and spring minimum related to the seasonal variation in nearshore equatorward wind stress. It is hypothesized that the late summer maximum in nearshore poleward flow is related to an offshore maximum in equatorward flow which, itself, is driven by negative wind stress curl in the offshore region. This proposed forcing scenario is based upon simple correlations of the seasonal cycles and many of the dynamical aspects have not yet been fully justified (e.g., the forcing mechanism for the late summer maximum nearshore poleward flow).

In addition to the low frequency studies summarized above, a number of studies of the nearshore circulation have been conducted from moored current meters off the coasts of northern California, Oregon, Washington, and Vancouver Island. With few exceptions, these studies have focused on short time scale variability over the continental shelf and are thus not generally pertinent to the present study which emphasizes seasonal variability over the continental slope. However, one of the results of the shelf studies is worthy of mention here since

it has apparently provided much of the guidance for dynamical modelling (see section 3). The current meter records of *Collins et al.* [1968] and *Mooers et al.* [1976] suggest that the undercurrent over the shelf is highly coupled to the equatorward wind stress. These studies document events of strong upwelling favorable winds where the shelf response consisted of an intensification of the equatorward surface jet and poleward undercurrent. In the absence of upwelling, the shelf undercurrent disappeared. General conclusions drawn from these case studies may be misleading. Indeed, *Huyer et al.* [1974] observed an event where the response to strong upwelling was more nearly barotropic over the continental shelf and the undercurrent was not present. This is consistent with statistical analyses of 4 months of data in the summers of 1972 and 1973 at two locations on the Oregon shelf [*Kundu et al.*, 1975]. Over 90% of the variability over the shelf consisted of barotropic fluctuations in the alongshore velocity.

3. DYNAMICAL BACKGROUND

A thorough review of existing models of eastern boundary current systems is beyond the scope of this paper. A comprehensive summary of two-dimensional models can be found in *Allen* [1980]. This study focuses particular attention on the nearshore undercurrent over the continental slope. Models of this feature require the presence of a poleward pressure gradient and therefore must be fully three-dimensional. Summaries of early three-dimensional models of eastern boundary current systems are given in *O'Brien et al.* [1977] and *McCreary* [1981]. Most models examine the dynamical response of stratified eastern boundary regions to zonally uniform equatorward wind stress. This forcing mechanism has apparently been isolated because of the observational results of *Collins et al.* [1968] and *Mooers et al.* [1976] mentioned in section 2 which suggest that undercurrents are coupled to coastal upwelling. (Note however, from the earlier discussion, that this forcing mechanism may not be the most appropriate one.) Some models include bottom slope and most models restrict the winds meridionally. All of the models produce an equatorward surface jet and poleward undercurrent in response to equatorward wind stress.

The coastal wind-generated response in a flat bottom stratified ocean propagates poleward in the form of baroclinic Kelvin waves. These Kelvin waves become coastal trapped waves (a hybrid of barotropic continental shelf waves and baroclinic Kelvin waves) in the presence of both stratification and bottom slope [*Wang and Mooers*, 1976; *Clarke*, 1977; *Huthnance*, 1978]. A steady state balance between alongshore wind stress and alongshore pressure gradient is established after passage of the poleward propagating coastal trapped waves. Since the propagation speeds of coastal trapped waves are rapid (on the order of 2 m/s for the lowest order baroclinic mode), the coastal steady state balance is achieved rather quickly.

The offshore scale of coastal response to alongshore wind stress in a flat-bottom f plane model is only about 30 km (the Rossby radius of deformation). Because of the β effect, the coastal response to the sudden onset of steady winds disperses into Rossby waves and spreads offshore [*McCreary*, 1976]. Thus, the width of the coastal response depends on the time elapsed after a wind stress is applied. Neglecting frictional effects, the steady state Sverdrup balance between vertically integrated meridional velocity and wind stress curl is established in the wake of the westward propagating Rossby waves. The time required to achieve this steady state is much longer than the coastal steady state balance because of the slow Rossby wave propagation speeds (about 1–2 km/day for the lowest order baroclinic mode).

These dynamical concepts are nicely summarized in the linear steady state model of *McCreary* [1981]. The response of a continuously stratified flat bottom ocean to steady equatorward alongshore wind stress is given as an expansion of vertical normal modes. The high-order baroclinic modes are characterized by a two-dimensional balance between onshore geostrophic transport and offshore Ekman transport from the equatorward wind stress. Their sum produces the cross-shore circulation characteristic of coastal upwelling. The low order baroclinic modes propagate poleward very quickly and establish a balance between the equatorward wind stress and a poleward pressure gradient. For winds without curl this is a state of rest with no meridional flow. It is thus the intermediate baroclinic modes which contribute the most to the alongshore flow. These modes have equatorward flow near the surface with flow reversals at depth which result in an undercurrent. The effects of wind stress are confined to the upper mixed layer. However, the poleward pressure gradient established in the wake of the poleward propagating low-order baroclinic modes extends deep in the water column and can be viewed as the driving force for a poleward flow beneath the mixed layer (the undercurrent). The onshore geostrophic flow associated with the poleward pressure gradient "feeds" the undercurrent.

Nearly all models of the undercurrent have been limited to studies of the response to steady wind forcing. Recently, *Philander and Yoon* [1982], hereinafter referred to as PY, have studied the response of a nonlinear, continuously stratified, flat bottom ocean with a meridional coastline to periodic alongshore wind stress. The winds in this model are meridionally restricted but otherwise uniform, both meridionally and zonally. Results are presented for 20- and 200-day wind forcing and qualitative discussion is given of the features that would be present for longer period wind forcing.

Fluctuating winds induce a coastal response with offshore structure which depends on the time scale of the variable winds. At low frequencies the coastal response spreads offshore which can result in a complex system of poleward and equatorward flows along any cross-shore section. At high frequencies, Rossby wave propagation is no longer possible, and the response to alongshore wind stress remains trapped at the coast. The cutoff frequency varies with latitude; for any given frequency each baroclinic mode has an associated critical latitude north of which Rossby wave propagation is not possible. For a baroclinic mode with poleward phase speed c, the critical latitude is given by [see *McCreary*, 1977]

$$\Theta_{cr} = \tan^{-1}\left[\frac{c}{2R_e\omega}\right]$$

where $R_e = 6.4 \times 10^6$ m is the radius of the earth and ω is the frequency of the forcing. For a phase speed of 2 m/s, the critical latitude for annual wind forcing is about 38°N (the latitude of San Francisco) and the critical latitude for semiannual forcing is about 21°N.

The PY model domain ranges from 0° to 30°N and therefore does not strictly apply to the region off central California which is located at about 35°N. However, the principle model results would not be expected to differ qualitatively at higher latitudes for wind forcing at low enough frequencies. Although some of the model features are unrealistic (in particular, the simple bottom topography, meridional wind stress restricted

to the region between 10° and 20°N and the lack of a nearshore wind stress curl), this is the only model to date which examines the response to periodic wind forcing. It therefore forms the primary basis for qualitative comparison with the observations of seasonal variability presented in this study.

The nearshore shallow equatorward surface jet and poleward undercurrent characteristic of eastern boundary regions develop in the PY model during the equatorward cycle of 200-day periodic alongshore wind stress. Both extend well north of the region of wind forcing due to Kelvin wave propagation. The phase relations between time variability of wind stress, alongshore pressure gradient, and meridional velocity in the PY model provide useful diagnostic features. These phase relations were first discussed by *McCreary* [1977]. They depend on latitude, the frequency of wind forcing, and mixing. For very long-period wind forcing, the alongshore pressure gradient varies in phase with the wind stress. If there is no mixing, the alongshore surface velocity leads the pressure gradient (and hence the wind stress) by one quarter of a period at low latitudes. The undercurrent (which is 180° out of phase with the surface flow) then lags the pressure gradient by one quarter of a period. As latitude increases (or the period of wind forcing decreases), the phase lead of the surface velocity decreases and the phase lag of the undercurrent increases.

For 200-day wind forcing, the PY model results indicate that the alongshore pressure gradient varies in phase with the wind stress. The alongshore surface velocity leads the pressure gradient and wind stress by about 25 days, and the poleward undercurrent then lags the pressure gradient by about 75 days. For higher latitudes (such as those relevant to this study) the phase lead of the surface velocity would decrease and the phase lag of the undercurrent would increase.

The restriction to zonally uniform meridional wind stress could be an important weakness of eastern boundary current models. It is known that there are strong cross-shore gradients in the wind stress in these regions, resulting in a nearshore positive wind stress curl (see Figure 6). *Pedlosky* [1974] examined the response of eastern boundary regions to steady but otherwise arbitrary winds over a sloping bottom. He showed that equatorward winds drive a baroclinic equatorward surface jet but that an undercurrent need not appear as a necessary consequence of upwelling. A nearshore positive wind stress curl forces a poleward barotropic flow. Depending on the strength of equatorward wind stress at the coast, this barotropic flow may be overridden by the baroclinic equatorward surface jet resulting in an undercurrent. To the extent that equatorward winds at the coast are correlated with the nearshore positive wind stress curl, the undercurrent may be correlated with coastal upwelling.

4. CalCOFI Data Description

The data used here to examine geostrophic velocity in the California Current are drawn from the CalCOFI hydrographic data base. The temporal sampling of these data has been somewhat irregular for the past 33 years. Monthly surveys on a geographically fixed grid system began in 1950 and continued through 1960 with few interruptions. Surveys were reduced to quasi-quarterly (nominally January, April, July, and October) beginning in 1961. This sampling strategy was maintained through 1968, after which sampling was changed to monthly coverage every third year (1969, 1972, 1975, 1978, and 1981). The 1981 data have not yet been fully processed so the analysis here includes only the 23 CalCOFI-sampled years between 1950 and 1978.

Spatial sampling of CalCOFI hydrographic data is based on parallel lines separated by 65 km extending seaward approximately perpendicular to the southern California coast. The full CalCOFI sampling region ranges from the U.S.-Canadian border to the southern tip of Baja California. The station spacing along each line is also 65 km with somewhat tighter spacing over the continental shelf and slope. Not all hydrographic stations in this geographically fixed grid pattern were occupied during any given sample month. The region surveyed most frequently extends approximately 300–400 km offshore and ranges from San Francisco to southern Baja California. Lines spaced 195 km apart (designated "cardinal" lines) were occupied more frequently than the intermediate "ordinal" lines.

There are a number of obvious limitations imposed by the coarse spatial and intermittant temporal sampling of the CalCOFI data and the possible aliasing of higher frequency variability in the monthly observations. Nevertheless, the more than 18,000 hydrographic profiles collected between 1950 and 1978 can provide useful information on low frequency variations in the flow in the southern California Current System. There are no other data sets (e.g., direct current measurements) in this region which can address the time scales of interest here. Horizontal maps and vertical sections of hydrographic data collected during each individual CalCOFI cruise and summaries of the seasonal variability have been published by CalCOFI as part of a series of physical and biological atlases (see *California Cooperative Oceanic Fisheries Investigations*, 1963; *Wyllie*, 1966; *Wyllie and Lynn*, 1971; *Eber*, 1977; *Lynn et al.*, 1982].

In this study, attention is focused on the seasonal variability along lines 70 and 80 in the northern half of the intensely sampled CalCOFI domain (see Figure 1). These two lines extend offshore from Point Sur and Point Conception, respectively. This choice was based on the relatively simple bottom

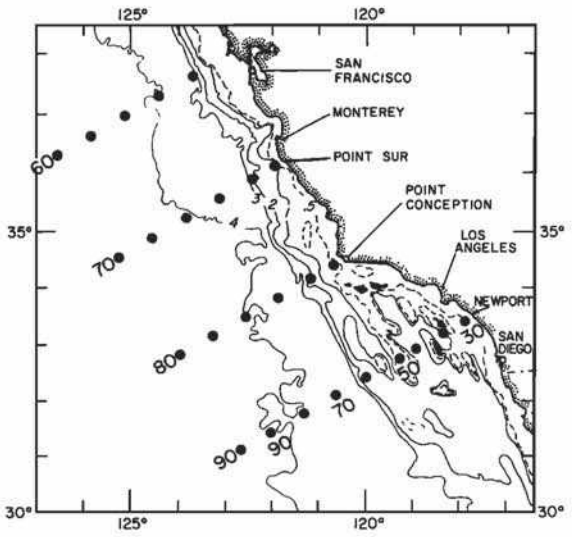

Fig. 1. Map of the central California Current region showing bottom topography (contours in km) and key geographical locations along the coast. The dots show the hydrographic stations along the CalCOFI "cardinal lines" that lie in water deeper than 500 m and were occupied 40 or more times between 1950 and 1979. (There are additional stations in the nearshore region, but they do not satisfy these two criteria. Stations along intermediate "ordinal lines" with 40 or more observations are also not shown.) The line numbers are labeled at the offshore end of each line, and station numbers are labeled along line 90.

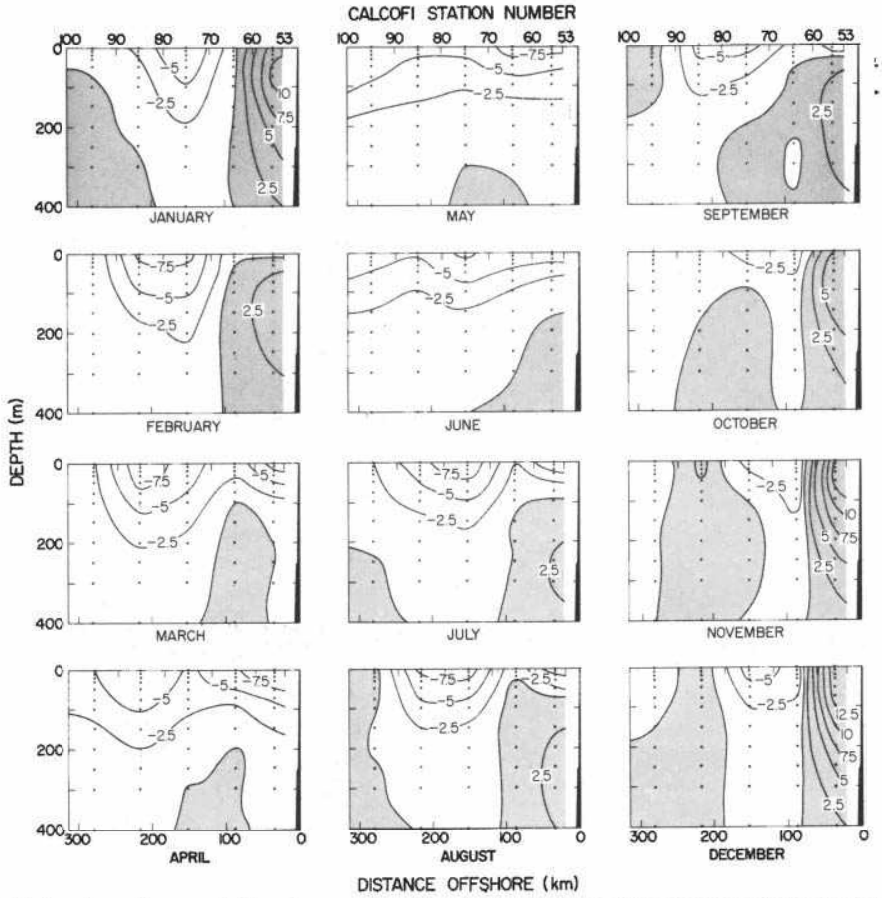

Fig. 2. Vertical sections of seasonal alongshore geostrophic velocity relative to 500 dbar along CalCOFI line 70 off Point Sur. Shaded regions correspond to poleward flow.

topography and predominantly alongshore flow in the region north of Point Conception. In comparison, the average flow in the southern region shows a permanent meander at 31°N with strong eastward flow approaching very near the northern Baja coast. This feature has been confirmed from drifter measurements by *Reid et al.* [1963]. It may be a response to the localized negative wind stress curl found in this region (see Figure 6) as suggested by *Bakun and Nelson* [1977] and *Hickey* [1979] or it may be topographically induced by the Channel Islands and seamounts which extend southeastward from Point Conception. Present dynamical models might not be expected to account accurately for the flow field in this region of possibly strong topographic or wind stress curl influence.

The method used to determine the seasonal variability of geostrophic velocity is discussed in detail in the appendix. Briefly, seasonal dynamic heights were computed relative to 500 dbar at 13 standard depths from the sea surface to 500 m for each CalCOFI grid point. The alongshore component of seasonal geostrophic velocity relative to 500 dbar was then computed at the 13 standard depths through the geostrophic relation by finite differencing seasonal dynamic heights between neighboring stations along each CalCOFI line. The reliability of these seasonal geostrophic velocities is discussed in the appendix. The choice of 500 dbar as a reference level was dictated by the fact that relatively few of the CalCOFI hydrocasts extend deeper than 500 m. However, at stations where deeper measurements were made, the dynamic height relative to 500 dbar generally differed from that computed relative to 1000 dbar by less than 5 mm (which corresponds to less than 1 cm/s velocity error for 65 km station spacing).

It should be noted that geostrophic velocities computed from this coarse station spacing (generally 65 km with 32.5 km spacing between the nearest inshore pair of stations) tend to be somewhat smoothed versions of the actual flow field. Velocities are underestimated in regions where the flow consists of a narrow jet. Decreasing the station spacing would increase the resolution, but then the velocity estimates become more sensitive to observational errors in temperature, salinity, and pressure in the hydrocasts. The CalCOFI grid spacing appears to be a reasonable compromise between spatial resolution and data reliability for the time and space scales of interest in this study.

As a final note concerning data, velocity values relative to 500 dbar can be directly computed only between stations in water deeper than 500 m. For stations in shallower water, estimates of velocity relative to 500 dbar can be obtained by extrapolation from deeper water by using any of a number of techniques. These extrapolations can give reasonable results for nearshore dynamic height [*Reid and Mantyla*, 1976; *Huyer*, 1980], but their accuracy for geostrophic velocity has not yet been demonstrated. Accuracy of the extrapolation technique for dynamic height does not imply that the method is also accurate for velocity extrapolations; small errors in dynamic height can lead to very large errors in geostrophic velocity. Rather than introduce possible errors and draw misleading conclusions from the extrapolation technique, the relative velocities examined here were computed only between

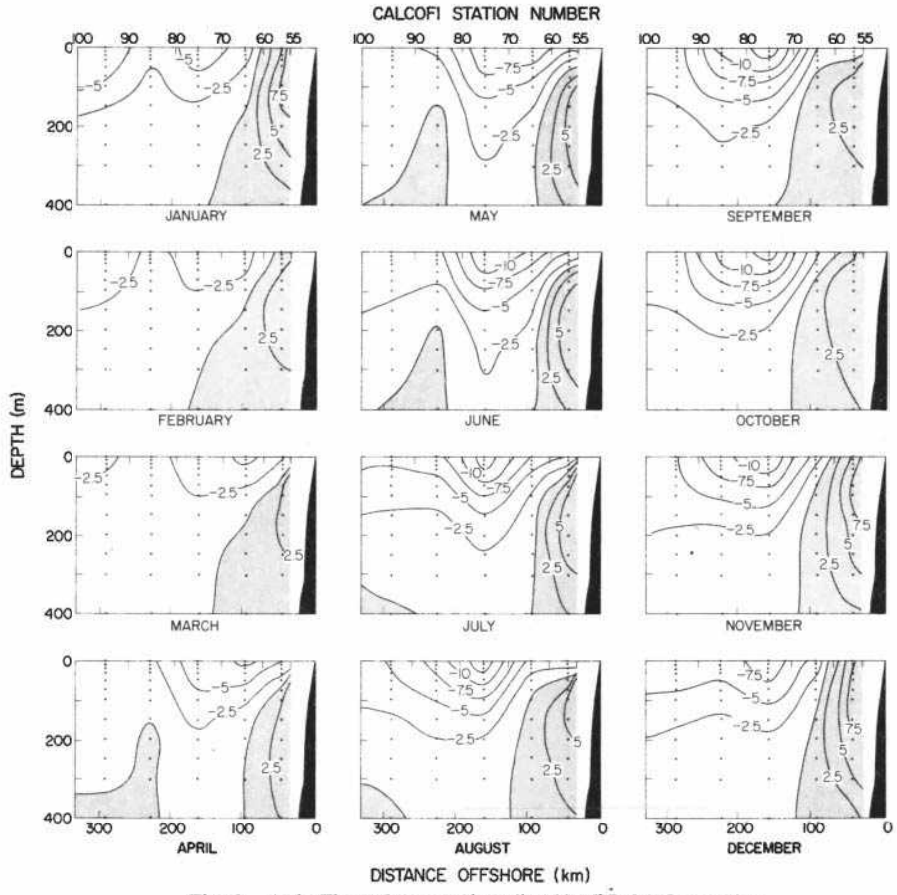

Fig. 3. As in Figure 2 except along line 80 off Point Conception.

stations in water deeper than 500 m. Thus, this study does not consider the flow on the continental shelf or upper continental slope.

5. Description of Seasonal Alongshore Velocity

The seasonal variability of alongshore geostrophic velocity relative to 500 dbar along a vertical section off Point Sur (line 70 in Figure 1) is shown in Figure 2. All of the well-known features of the California Current system are easily identifiable. The core of the equatorward California Current is located between 100 and 200 km offshore and is mostly restricted to the upper 200 m. The seasonal variability of this core shows two equatorward maxima per year with peak velocity of 9 cm/s in February–March and again in July–August. (The core is displaced slightly farther offshore in the wintertime maximum.) During March–April and July–September there is a narrow second maximum equatorward flow very nearshore with velocities of 5–8 cm/s. This jet may be even more intense over the continental shelf, but this region is not adequately sampled with the CalCOFI data. The existence of both nearshore and offshore equatorward flow maxima has been noted previously by *Hickey* [1979].

The undercurrent off Point Sur is confined to the continental slope region within 75–100 km of the coast. This nearshore poleward flow at depth is absent March–May. It first appears in June–July and is present through February. The poleward flow extends all the way to the surface from October through February (the Davidson Countercurrent) with a maximum poleward velocity at the surface in December (14 cm/s). During the remainder of the year the maximum poleward flow is below the surface. It should be kept in mind that the undercurrent in this figure has zero velocity at 500 m because of the choice of 500 dbar as a reference level for the geostrophic calculations. While the seasonal velocities are certainly small at this depth, there is no assurance that they are zero. The undercurrent may be broader or narrower at greater depths.

Vertical sections of the seasonal alongshore geostrophic velocity relative to 500 dbar off Point Conception (line 80 in Figure 1) are shown in Figure 3. The flow differs from that off Point Sur in a number of major respects. The core of the California Current is again located 100–200 km offshore and mostly limited to the upper 200 m, but there are not two seasonal maxima as there are off Point Sur. Instead, the equatorward flow remains strong from June through October with a relatively steady maximum velocity of 14 cm/s. This equatorward flow is weakest in February–March, a time period which coincides with one of the maxima in the flow off Point Sur. There is no evidence of the secondary equatorward jet over the continental slope found off Point Sur. Again, it is possible that an equatorward jet exists over the continental shelf, but it cannot be detected from this data set.

The most interesting feature in the flow off Point Conception is the undercurrent. The poleward flow is confined to the nearshore 75–100 km as it is off Point Sur. However, the undercurrent off Point Conception is poleward all year and distinctly semiannual with maxima in June and December (velocities of 6 and 8 cm/s, respectively). As is the case off Point Sur, the poleward flow extends to the surface from October

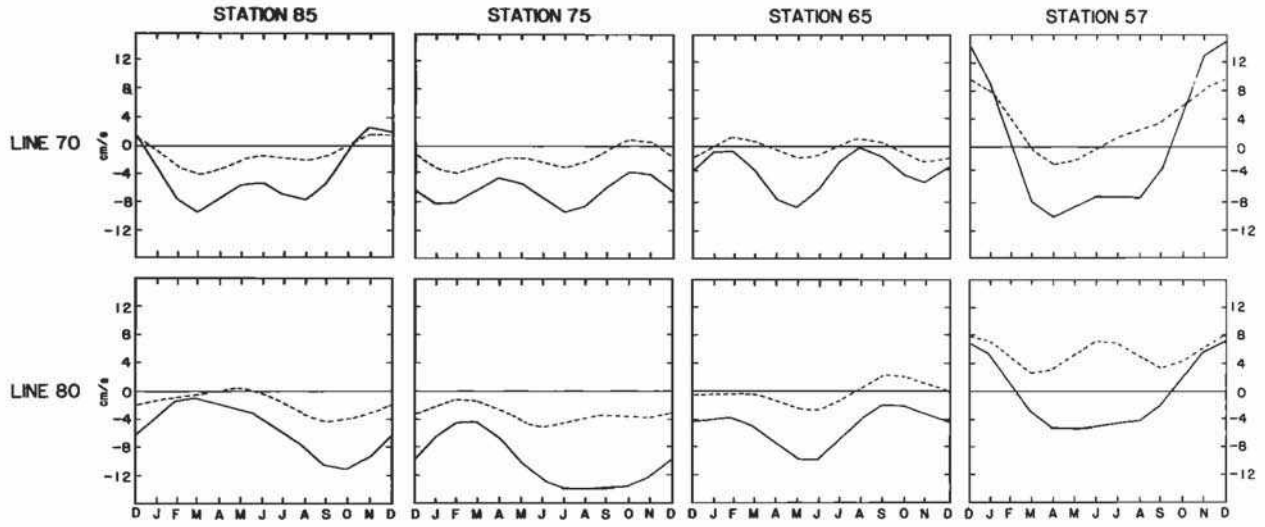

Fig. 4. Seasonal time series of alongshore geostrophic velocity at the surface (solid lines) and at 150 dbar (dashed lines) relative to 500 dbar between each station pair along CalCOFI lines 70 and 80 (see Figure 1).

through February (the Davidson Countercurrent). Off Point Conception the maximum poleward velocity is located subsurface throughout the year.

The temporal variations of the features described above are somewhat more easily seen from time series at fixed locations. The seasonal cycles of geostrophic velocity relative to 500 dbar at the surface and at 150 m depth between each pair of stations along lines 70 and 80 are shown in Figure 4. At the three offshore stations along both lines, there is strong vertical coherence in the seasonal flow. That is, when the equatorward flow at the surface weakens, it also weakens at 150 m. At the inshore station off Point Sur (station 70.57) the surface and 150 m geostrophic velocities are also quite coherent with maximum equatorward velocity in April and maximum poleward velocity in December. In comparison, there is strong vertical shear in the flow at the inshore station off Point Conception; the surface flow is predominantly annual while the flow at 150 m is almost purely semiannual. This significant difference cannot be attributed to any sampling problems because the velocities at the two depths were computed from exactly the same collection of monthly observations (see appendix). The summer maximum in the subsurface poleward velocity off Point Conception is apparently a very real and recurring feature; it was observed in every June and July sample from 1950 to 1979 (see the distribution of raw observations in Figure 8*b* of the appendix). In contrast, the undercurrent off Point Sur was never observed in June, and only weak poleward flow has ever been observed in July (see Figure 8*a*).

The flow over the continental slope is the most intriguing because of the complete seasonal reversal of the surface velocity and the subsurface poleward flow in opposition to the generally equatorward California Current. This is the area where dynamical models stand the greatest chance of being successful; the flow in the region farther offshore is likely to be a very complex superposition of local wind-generated response, eddies and meanders, and velocity fluctuations associated with westward propagating Rossby waves. The remainder of this paper restricts attention to the flow over the outer continental slope (defined here to be that part of the slope in water deeper than 500 m).

Because the alongshore velocity structure over the continental slope off Point Sur is so distinctly different from that off Point Conception less than 200 km to the south, it is of interest to examine the alongshore continuity of the nearshore flow in a larger-scale sense. The CalCOFI data set is somewhat limiting in this respect. The seasonal geostrophic velocity at the surface and at 150 m is shown in Figure 5 at selected locations over the outer continental slope ranging from San Francisco to San Diego. These particular stations were chosen on the basis of a somewhat arbitrary criterion for data sampling distribution: These are all of the nearshore CalCOFI station pairs with 40 or more dynamic height observations over the 30-year period from 1950 to 1979. Station pairs with fewer observations were rejected because of insufficient data to resolve reliably the seasonal variability. The CalCOFI station pairs used to compute these geostrophic velocities are summarized in Table 1.

It is evident from Figure 5 that, at all locations over the outer continental slope except off Point Conception (station 80.57), the geostrophic velocity at the sea surface is highly coherent with that at 150 m. There appear to be two distinct flow regimes. The two southern stations (inside the Southern California Bight) show predominantly semiannual variability with maximum poleward flow in June and November–December and maximum equatorward flow (or minimum poleward flow) in March and September. Semiannual variability in the Southern California Bight has been noted previously by *Tsuchiya* [1980] from hydrographic data collected during nine cruises between 1974 and 1977 [see, also, *Hickey and Pola*, 1983, Figure 5]. In that earlier study, Tsuchiya suggested that the semiannual variability may have been an artifact of insufficient data sampling. However, the results presented here indicate that semiannual variability is a real and recurring feature in the Southern California Bight. (The phase difference between the semiannual signal noted by Tsuchiya and that presented here is likely due to sampling limitations from the 3-year Tsuchiya data set; alternatively, the phase shift may be because Tsuchiya describes variability over the continental shelf, whereas this study examines variability over the outer continental slope.)

The second flow regime is located in the far northern region of Figure 1. The two northern stations also show predomi-

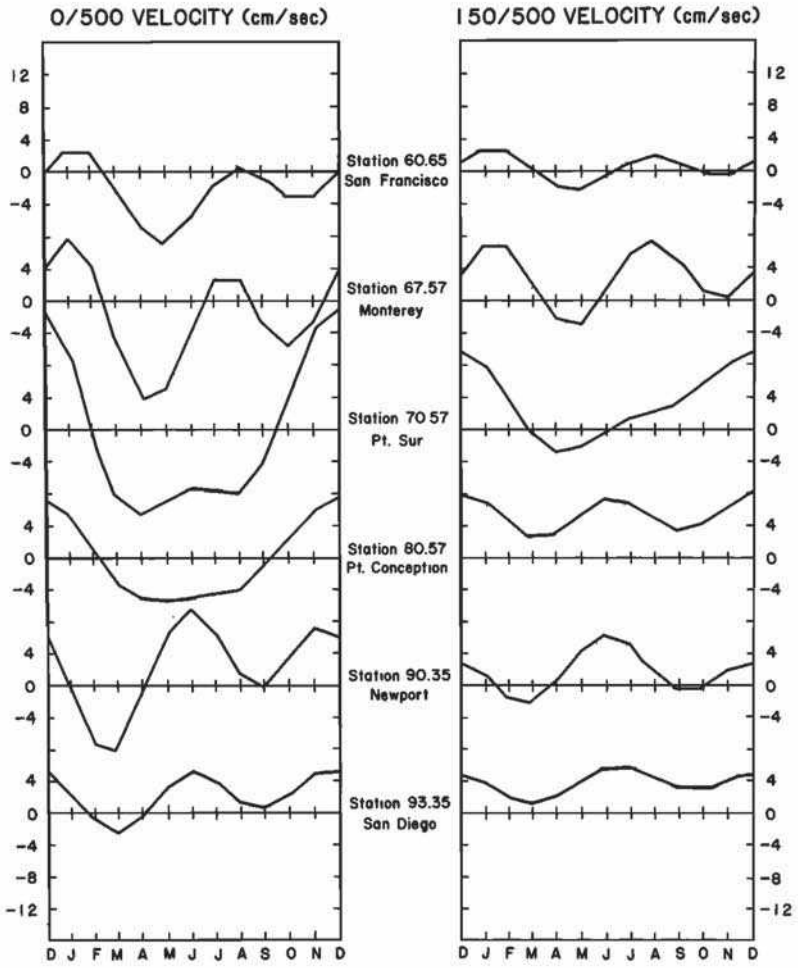

Fig. 5. Seasonal time series of alongshore geostrophic velocity at the surface and at 150 dbar over the outer continental slope (the nearest inshore pair of stations in water deeper than 500 m) from San Francisco to San Diego. These are all of the nearshore CalCOFI station pairs in this region with 40 or more observations from 1950 to 1979. The actual CalCOFI station pairs used to compute these geostrophic velocities are summarized in Table 1.

nantly semiannual variability, similar to the Southern California Bight flow regime, but with maxima and minima phase shifted 1–2 months later than those in the southern regime. This phase shift is suggestive of poleward propagation of the semiannual variability. However, there is no evidence for systematic poleward phase propagation as would be expected from simple dynamical arguments. Instead, the region between Point Sur and Point Conception appears to be a sudden transition region between the two separate semiannual regimes. The nearshore surface flow along lines 70 and 80 is very different from that to either the north or south as is the undercurrent along line 70. A noteworthy feature in Figure 5 is that, although the undercurrent along line 80 is not coherent with the surface flow, it is coherent with flow throughout the water column in the Southern California Bight.

6. Discussion

Before comparing the seasonal geostrophic velocity described in section 5 with the theoretical work of PY, it is important to emphasize the limitations of testing dynamical models from analysis of seasonal cycles. It is well known that the presence of any narrow band signal (e.g., tidal cycle or seasonal cycle) significantly reduces the number of independent samples in a time series [see, e.g., *Chelton*, 1982]. Correlations between two seasonal cycles are not very meaningful since they are based on only a very small number of degrees of freedom. Anything less than nearly perfect correlation will not be statistically significant. The best method for examining the relation between two geophysical quantities is to remove the seasonal cycles from both time series and look for correlations in the residual "anomalies." Unfortunately, the CalCOFI data are too gappy to resolve adequately the anomalous variability of geostrophic velocity so that only seasonal variability is discussed here.

The approach taken here is not to test rigorously the model of PY but rather to look for qualitative consistency between the model results and calculated seasonal geostrophic velocities over the outer continental slope. The goal is to identify strengths and weaknesses in the dynamical theory, thereby hopefully providing some guidance for future modelling efforts. More quantitative statistical tests of dynamical models are best conducted from (presently nonexistent) long time series of current velocity from moored current meters.

From the discussion in section 3, dynamical models suggest that the flow over the continental shelf and slope is driven by the wind stress (both local winds and winds at locations farther south). To summarize briefly, we expect a poleward pressure gradient to fluctuate seasonally in phase with the along-

shore wind stress. The alongshore surface velocity should lead the equatorward wind stress and poleward pressure gradient by somewhat less than one quarter of a period (approximately 3 months for the annual cycle and 1½ months for the semiannual cycle). The poleward pressure gradient drives a poleward undercurrent which varies 180° out of phase with the surface flow. This poleward subsurface flow should therefore lag the poleward pressure gradient and wind stress by somewhat greater than one quarter of a period.

The detailed temporal and spatial characteristics of the wind field over the California Current are not well understood. Probably the best description of the seasonal winds in this region is that given by *Nelson* [1977]. He compiled direct ship observations of wind vectors by 1° square areas from records dating back to the mid-19th century. The resulting long-term average wind stress for July is shown in Figure 6. The spatial structure of the wind field is similar throughout the year, but the magnitude changes seasonally. (North of San Francisco, the wind direction also changes seasonally.) In the region examined in this study, the winds are highly coherent in the alongshore direction. They blow equatorward and parallel to the coast year round with maximum intensity in May. Although most models consider only zonally uniform wind stress, it is noteworthy that the winds over this region of the California Current appear to be strongest approximately 200 km offshore so that there is a nearshore positive wind stress curl year round (see Figure 6). The magnitude of this wind stress curl varies seasonally approximately in phase with the alongshore wind stress.

The seasonal cycles of alongshore geostrophic velocity at the surface over the outer continental slope off Point Sur and Point Conception are reproduced from section 5 as the top curves in Figure 7. The curves in the centers of the panels are the seasonal cycles of local wind stress (solid lines) and wind stress curl (dashed lines) at these two geographical locations. These cycles were computed from spatial averages of the *Nelson* [1977] 1° long-term averages (see figure caption). Since these winds have not been subjected to the same harmonic analysis as the hydrographic data (see appendix), comparison of these seasonal cycles with the seasonal geostrophic velocity must be interpreted with some caution. However, visual inspection of Figure 7 suggests that the surface velocity leads the wind stress by about 1 month. The maximum equatorward surface flow occurs in April at both locations which is one month earlier than the maximum equatorward wind stress. Similarly, the maximum poleward surface flow occurs in December at both locations, which is one month earlier than the minimum equatorward wind stress. Somewhat more quantitative analysis indicates maximum correlations of 0.96 at Point Conception with no lag and 0.91 at Point Sur with 1-month lag of the wind stress. (No attempt will be made here to determine the significance level of these correlations [see *Chelton*, 1982].)

TABLE 1. CalCOFI Stations Used to Compute the Nearshore Geostrophic Velocities Shown in Figure 5

Location	CalCOFI Line	Inshore Station	Offshore Station	Separation, km
San Francisco	60	60	70	65
Monterey	67	55	60	32.5
Point Sur	70	54	60	39
Point Conception	80	55	60	32.5
Newport	90	32	37	32.5
San Diego	93	30	40	65

See Figure 1 for station locations.

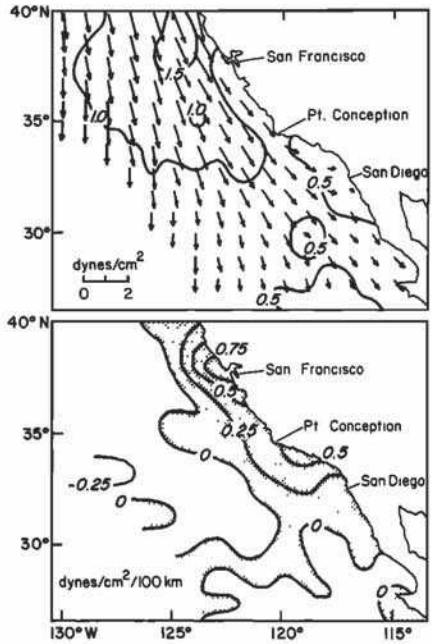

Fig. 6. Long-term average wind stress (top) and wind stress curl (bottom) for the month of July. Shaded regions in bottom figure correspond to positive wind stress curl. Maps constructed from 1° averages of 100 years of ship observations compiled by *Nelson* [1977].

This approximate 1-month phase lead is somewhat shorter than expected but is otherwise in qualitative agreement with the phase relations predicted by the model of PY. As discussed in section 3, the shorter phase lag may be because the geographic region examined here is somewhat north of the region for which the PY solutions were derived. Alternatively, the discrepancy may be due to the different methods of computing the seasonal cycles. Note, however, that the surface velocity is poleward from October through February at both locations (the Davidson Current) which is in opposition to the overlying wind stress. This time period coincides with the time of weakest equatorward winds and maximum poleward undercurrent. The PY model considers only oscillatory wind stress. Since the model is nonlinear, it is difficult to anticipate the response that would be generated by more realistic wind forcing consisting of seasonal oscillations about a mean equatorward wind stress. However, it seems unlikely that the model could account for a surface flow in opposition to the wind stress without including the effects of wind stress curl.

From section 3, the alongshore pressure gradient should be important to the dynamics of the undercurrent. The total pressure gradient consists of a barotropic and a baroclinic contribution. For a meridional coastline parallel to the y axis, the total alongshore pressure gradient at a depth D (positive z upward) is given by

$$\frac{\partial p}{\partial y} = \rho_0 g \frac{\partial h}{\partial y} + g \int_D^0 \frac{\partial \rho}{\partial y}\, dz$$

where p is the pressure, g the gravitational acceleration, h the sea surface elevation, ρ the water density, and ρ_0 the surface water density. At the 150 m depth of interest here, there is very little seasonal variability of the alongshore density gradient in

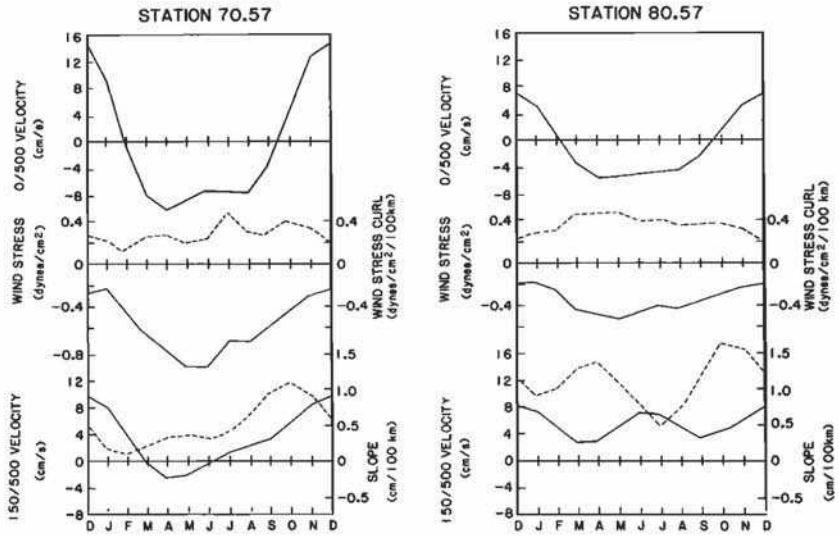

Fig. 7. Seasonal time series over the outer continental slope off Point Sur (left) and Point Conception (right) of alongshore geostrophic velocity at the surface (top solid curve); wind stress curl (top dashed curve); alongshore wind stress (middle solid curve); 150 dbar alongshore geostrophic velocity (bottom solid curve); and alongshore pressure gradient (bottom dashed curve). The wind stress and wind stress curl seasonal cycles were computed by averaging the *Nelson* [1977] long-term average ship observations over three grid points in the alongshore direction, centered over the nearshore region off Point Sur and Point Conception.

this region of the California Current (see seasonal average alongshore sections of density in *Lynn et al.* [1982]). Therefore, the seasonal variability of the total pressure gradient is dominated by the barotropic component from the alongshore sea level slope.

The lower curves in Figure 7 show the 150 m geostrophic velocity over the outer continental slope off Point Sur and Point Conception (solid lines) and an estimate of the barotropic component of the local alongshore pressure gradient (dashed lines). These measures of alongshore barotropic pressure gradient were computed by differencing the seasonal dynamic height of the sea surface relative to 500 dbar over the outer continental slope along neighboring cardinal lines to the north and south. For station 70.57, the seasonal barotropic pressure gradient was computed from differences in dynamic height between stations 60.60 and 80.60 (see Figure 1). For station 80.57, the barotropic alongshore pressure gradient corresponds to differences in dynamic height between stations 70.60 and 90.60.

It is evident from these curves that the undercurrent and poleward pressure gradient are highly coherent with each other at both locations. Off Point Sur the undercurrent lags the poleward pressure gradient by 2 months. There is even a correspondence between the slight secondary maxima of both signals from the weak semiannual contribution to the seasonal variability. Off Point Conception, the undercurrent also lags the poleward pressure gradient by 2 months. There is a direct correspondence between both peaks of the semiannual variability including the asymmetry between the two maxima. These visual phase relationships are confirmed by maximum correlations of 0.97 and 0.80 at 2-month lag at Point Sur and Point Conception, respectively. Overall, the poleward pressure gradient is greater throughout the year off Point Conception which apparently accounts for the stronger poleward flow. In comparison, the poleward pressure gradient is considerably weaker during the winter off Point Sur which explains the weaker poleward flow during the spring (there is actually a slight reversal with 2 cm/s equatorward flow in April and May).

The close similarity between the velocity and pressure gradient seasonal cycles is very gratifying since all dynamical models indicate that the undercurrent is "driven" by the poleward pressure gradient. The 2-month phase lag between the pressure gradient and the undercurrent agrees reasonably well with the model results of PY. However, the driving force for the poleward pressure gradient cannot be determined from the analysis here; it does not appear to be very closely coupled to the local wind field in this region which shows little or no semiannual variability. And since the poleward pressure gradient is so different at the two locations, it is difficult to imagine how winds at locations to the south could be the driving force for the pressure gradients.

It is useful to compare the results presented here with those of *Hickey* [1979]. She determined the long-term seasonal variability of the undercurrent at widely spaced locations along the west coast of North America (no stations between Point Conception and Cape Mendocino, approximately 300 km north of San Francisco). It is evident from her figures that semiannual variability is a prevalent feature of the California Current System. This semiannual signal is more clearly defined in the harmonic seasonal cycles presented here. In addition, the alongshore continuity of the undercurrent has been examined here in much greater detail at six locations from San Diego to San Francisco (see Figure 5). The results are consistent with those of *Hickey* [1979] in the southern and northern semiannual regimes. However, the more closely spaced sampling indicates a lack of significant semiannual variability off Point Sur. The possibility that this may be an artifact of inadequate temporal sampling by the gappy CalCOFI hydrographic data cannot be ruled out (see appendix) but the evidence presented here suggests that, if it exists, the semiannual variability of the undercurrent off Point Sur is much weaker than elsewhere along the California coast. Another possibility that cannot be discounted from the 500 m hydrographic data

analyzed here is that semiannual variability may exist off Point Sur but is restricted to shallower water over the upper continental slope or shelf. This could best be determined from long-term current meter records.

Finally, it is also useful to compare the alongshore pressure gradients computed here with the recent work of *Hickey and Pola* [1983]. The long-term average barotropic pressure gradients computed from tide gauge sea level slope between San Francisco and Avila Beach (approximately 75 km north of Point Conception) and between Avila Beach and San Diego are presented in their Figure 5. The San Francisco–Avila Beach seasonal sea level slope is virtually identical to the Point Sur pressure gradient computed here from the CalCOFI hydrographic data. The Avila Beach–San Diego sea level slope is not directly comparable to the Point Conception pressure gradient presented here. With the complex bottom topography and coastline geography and the presence of a permanent cyclonic eddy in the Southern California Bight, the relevance of coastal sea surface elevation at San Diego to the dynamics of the large-scale undercurrent is not at all clear. Because of the strong horizontal shear in the currents in the Southern California Bight, a small east-west error in the choice of location for sea level can lead to a significant error in the estimate of the alongshore sea level slope which drives the undercurrent. For this study, sea surface elevation (estimated from dynamic height relative to 500 dbar) at a station just offshore from the Channel Islands (CalCOFI station 90.60) was used rather than a station inside the bight. This choice was motivated by a belief that the poleward pressure gradient beyond the Channel Islands and perpendicular to CalCOFI line 80 is most relevant to the dynamics of the undercurrent at Point Conception. Indeed, the existence of a semiannual pressure gradient in this region of a semiannual undercurrent to some extent confirms this belief.

7. Summary and Conclusions

Twenty-three years of hydrographic measurements were used in section 5 to describe the seasonal geostrophic velocity relative to 500 dbar along two sections off central California (one off Point Sur and the other off Point Conception). Because of data limitations, attention has been limited to the region seaward of the outer continental slope (defined here to be water deeper than 500 m). The most interesting region along these two sections is the inner 100 km where there is a poleward undercurrent and a seasonal reversal in the surface flow. These poleward flows are generally limited to the region between the nearest inshore pair of CalCOFI stations in water deeper than 500 m along each line and are therefore barely resolved by the data. The nearshore surface flow is very similar at both locations with equatorward flow from March through September and poleward flow from October through February (the Davidson Current).

A rather surprising result of this study is the significant difference in the undercurrent at these two locations. Off Point Sur the deep flow is coherent with the surface flow but the surface and subsurface flow are distinctly different off Point Conception. At this more southerly location, both the surface and subsurface flow have a peak poleward velocity in December. However, there is a second peak poleward velocity at depths greater than 100 m in June when there is strong equatorward flow at the surface. There is some indication that this early summer undercurrent off Point Conception is related to flow throughout the water column inside the Southern California Bight (see Figure 5), suggesting that it may be topographically generated. From the data analyzed here, there is no evidence for a summer undercurrent off Point Sur less than 200 km to the north where there is weak equatorward flow in late spring and early summer.

The fate of this early summertime poleward flow after it turns north around Point Conception cannot be determined from the CalCOFI data. However, since there is no evidence of strong, early summer poleward flow off Point Sur, the results presented here would suggest that there is a subsurface convergence somewhere between Point Sur and Point Conception. It would be very interesting to have more early summer hydrographic sections in this region to determine whether this convergence exists and, if so, whether the response is non wind-related upwelling or offshore flow.

An attempt was made in section 6 to justify these seasonal variations in the flow over the outer continental slope from existing dynamical models. The only model to date which addresses temporal variability of three-dimensional eastern boundary currents is that of *Philander and Yoon* [1982]. It therefore formed the basis for the qualitative comparison between theory and observations in this study (in spite of some limitations of the applicability of the model).

The surface flow off both Point Sur and Point Conception appears to be coupled to the overlying wind field (which is very coherent in the alongshore direction). The phase relationship between the surface velocity and the wind stress is reasonably consistent with theory; equatorward surface velocity leads equatorward wind stress by about 1 month. The winds fluctuate with approximately an annual cycle but remain equatorward year round. However, the surface velocity is poleward (counter to the wind) in late fall and early winter. This behavior cannot be justified from the nonlinear PY model which examines the response to oscillatory forcing about a mean of zero. More realistic wind forcing will have to be considered to determine whether the PY model can account for the surface poleward Davidson Current. It may be necessary to include the effects of nearshore wind stress curl in the model as suggested by *Pedlosky* [1974].

Although the undercurrent is very different off Point Sur and Point Conception, it was found to be highly coherent with the local poleward pressure gradient at both locations. The phase relationship is in reasonable agreement with theory; poleward flow lags the poleward pressure gradient by about 2 months. The forcing mechanism for the poleward pressure gradient cannot be determined from these data. The model predicts that the presure gradient is related to the wind stress. However, the two bear very little resemblance to each other at either location. Generation of a seasonally varying poleward pressure gradient by propagation from lower latitudes is also an unlikely mechanism since the undercurrent (and pressure gradient) are so different off Point Sur and Point Conception.

An important result of this study is that the hydrographic data in this region of the California Current are quite "noisy" in the sense that the year-to-year variability is comparable in magnitude to variability over the seasonal cycle (see Figure 8). The nonseasonal variability is somewhat greater relative to the seasonal variability off Point Conception than off Point Sur. This "noise" is probably mostly geophysical in nature and should be viewed as a strength rather than a weakness. The limitations of testing dynamical models from statistical analysis of data with very strong seasonal cycles were discussed in section 6. The best test of dynamical models is with a highly variable system. Thus, Point Sur and Point Conception both

appear to be ideal locations at which to conduct long-term observational programs from moored current meters or a dense network of repeated hydrographic surveys.

APPENDIX: RELIABILITY OF THE SEASONAL CYCLES

Because of the intermittant spatial and temporal sampling of the CalCOFI hydrographic data (see section 4), the method of defining seasonal geostrophic velocity must be given careful consideration. The method used here was to compute first the seasonal dynamic height at each CalCOFI grid pont. Seasonal variability of dynamic height in the California Current system has been previously described by *Reid et al.* [1958], *Wyllie* [1966], *Hickey* [1979], and *Lynn et al.* [1982]. In these earlier studies, the seasonal cycles were determined by long-term averages of all available data for each calendar month. This method suffers from the disadvantage that the reliability of the seasonal mean values varies from month to month and from location to location, depending on the number of samples from which each monthly mean is constructed. As an example typical of the CalCOFI data set, station 55 on line 80 was occupied 14 times in January but only 4 times in December during the 30-year period from 1950 to 1979. The December mean value is clearly less reliable than the January mean value.

A more suitable method of determining the seasonal cycle from data characterized by such an uneven distribution of samples is to fit the time series of dynamic height to harmonics with annual and semiannual periods by least squares regression. This method has been used previously by *Lynn* [1967] to examine the seasonal variability of 10 m salinity and temperature in the California Current. Maps of dynamic topography determined from harmonic analysis [see *Chelton*, 1980] look very much like those produced by the long-term averaging method except that many of the eddy-like features (which are probably not recurring, year after year) are not present.

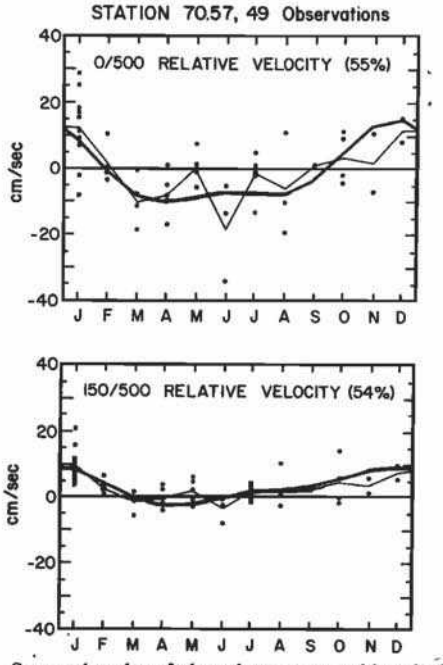

Fig. 8*a*. Seasonal cycles of alongshore geostrophic velocity at the surface and 150 dbar relative to 500 dbar over the outer continental slope off Point Sur. Heavy line corresponds to seasonal cycle computed from harmonic analysis of all available dynamic height data, and thin line corresponds to long-term averages of the raw geostrophic velocity observations (shown by the dots). Percentages of total variance accounted for by harmonic seasonal cycles are shown for each depth.

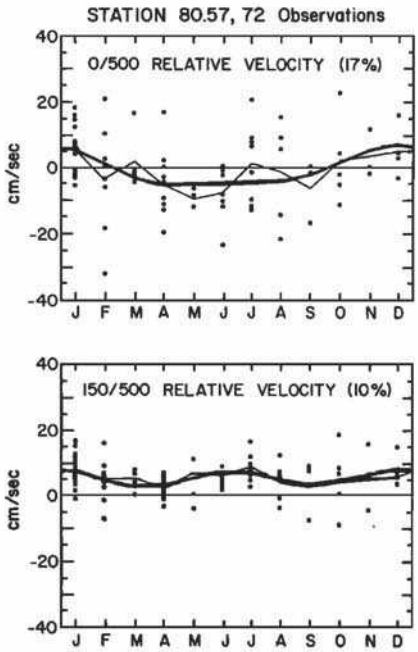

Fig. 8*b*. As in Figure 8*a* except over the outer continental slope off Point Conception.

The seasonal dynamic heights relative to 500 dbar were computed at 13 standard depths from the surface to 500 m by using this harmonic analysis method. Then the alongshore geostrophic velocities relative to 500 dbar were computed at each of the 13 standard depths through the geostrophic relation by finite differencing seasonal dynamic heights between neighboring stations. The resulting seasonal cycles are shown in Figures 2 and 3. the CalCOFI data are heavily biased toward January, April, July, and October surveys. The recent CalCOFI atlas by *Lynn et al.* [1982] presents vertical sections of long-term average relative geostrophic velocity for these 4 months. For these months that are well sampled by the CalCOFI data, the long-term average seasonal values do not differ significantly from the harmonic analysis seasonal values in Figures 2 and 3.

To illustrate the differences between long-term averaging and harmonic analysis methods of determining the seasonal variability, the harmonic seasonal geostrophic velocities at the surface and at 150 m over the outer continental slope along lines 70 and 80 are shown by the heavy lines in Figure 8. These are the seasonal cycles presented in Figure 7. The thin lines correspond to the seasonal cycles computed from long-term averages of raw geostrophic velocity values (shown by the dots). The limitations of the long-term averaging method are immediately apparent. This is particularly true for station 70.57 where the June long-term average is strongly influenced by a single observation of very large equatorward velocity. The November long-term average is similarly affected by an "anomalous" observation. The harmonic analysis method produced more reliable estimates of the seasonal values by effectively ascribing an equal number of degrees of freedom to each monthly estimate of the seasonal cycle. The tradeoff is that the harmonic analysis method forces smooth pictures of the seasonal variability which might, in some cases, obscure an interesting sudden change in the seasonal mean values due

to energy in higher-order harmonics. However, there is no evidence for seasonal recurrence of any such signals from the scattered raw observations in Figure 8, indicating that the harmonic analysis method is justified.

From Figure 8 it is also evident that the raw velocity values are highly variable. The magnitude of year-to-year variability for any particular month is about the same as that of the seasonal variability. The velocities off Point Conception are noisier than those off Point Sur; the harmonic seasonal cycle accounts for approximately half of the overall variability at station 70.57 and only 10–20% of the variability at station 80.57.

The motivation for computing seasonal geostrophic velocity from seasonal dynamic height rather than from harmonic analysis of raw geostrophic velocity was to utilize all available dynamic height observations. Each raw geostrophic velocity measurement requires dynamic height values at a pair of stations. The CalCOFI sampling strategy was such that it was not uncommon for only one of the stations in a pair to be sampled during a given cruise. For example, over the 30-year period from 1950 to 1979, station 80.55 was occupied 89 times and station 80.60 was occupied 99 times but there were only 72 months when both stations were occupied together. Similar sampling problems exist off Point Sur. Station 70.54 was occupied 56 times and station 70.60 was occupied 74 times but there were only 49 months when both stations were occupied. Computing seasonal dynamic height separately for each station rather than only from those monthly observations common to both stations maximizes the information content of the resulting seasonal cycles (and therefore, in some sense, maximizes the statistical reliability).

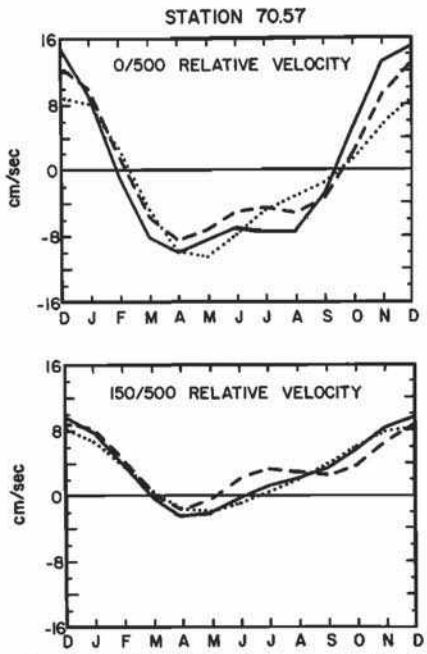

Fig. 9*a*. Seasonal cycles of alongshore geostrophic velocity at the surface and 150 dbar relative to 500 dbar over the outer continental slope off Point Sur computed by three different harmonic analysis methods. Solid line corresponds to harmonic analysis of all available dynamic height data at each of the inner two stations in water deeper than 500 m. Dashed line corresponds to harmonic analysis of only the 49 dynamic height observations coincident at both stations. Dotted line represents harmonic analysis of only the 34 dynamic height observations coincident at both the inner stations along line 70 and the two inner stations along line 80.

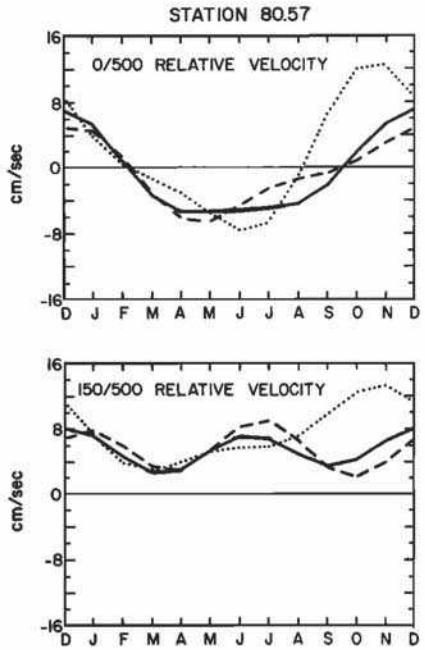

Fig. 9*b*. As in Figure 9*a* except over the outer continental slope off Point Conception. Dashed line is constructed from harmonic analysis of the 72 observations coincident at the two inner stations along line 80.

The stability of the seasonal geostrophic velocity computed from all available dynamic height can be examined by comparison with the alternative method computed from harmonic analysis of only those dynamic height monthly observations common to both stations in the pair (equivalent to harmonic analysis of the raw geostrophic velocity observations). The seasonal cycles computed by both methods are shown in Figure 9. There are minor differences (e.g., an increase in the magnitude of the semiannual constituent of the undercurrent off Point Sur), but they are not significant enough to alter the conclusions of this study. By either method, the semiannual constituent of the undercurrent off Point Sur is much weaker than that off Point Conception, while the surface flow is very similar at both locations.

A final concern that should be addressed is whether the apparent differences in the seasonal variability of the undercurrent off Point Conception and Point Sur are due to sampling problems. The seasonal cycles described in section 5 were computed from different months along each of the two CalCOFI hydrographic lines. There are only 34 months of coincident geostrophic velocity measurements between the inner pairs of stations along both lines 70 and 80. This is clearly not enough samples to define adequately the seasonal cycle with the high degree of variability characteristic of geostrophic velocity in the California Current (see Figure 8). However, it is useful to apply the harmonic analysis method to the 34 coincident raw geostrophic velocity measurements and compare the results along the two lines. These cycles are shown by the dotted lines in Figure 9. The seasonal cycles off Point Sur computed from only the 34 coincident observations are very similar to those computed from the other two methods. However, the seasonal cycles off Point Conception differ significantly from the other two seasonal cycles, indicating that the calculation is more sensitive to the data sampling at this location. This reflects the relatively greater degree of variability in the flow off Point Conception. It is nonetheless

evident that there are major differences in the flow off Point Conception and Point Sur, even computed from the subset of 34 observations. For example, in June and July there is no flow at 150 m off Point Sur while the flow is 5 cm/s poleward off Point Conception. Although analysis of the gappy CalCOFI data has not proven that the summer poleward flow is nonexistent off Point Sur, it appears to be much weaker than that off Point Conception, if it exists at all.

Thus, while sampling problems cannot be totally ruled out as a partial explanation for the differences in seasonal geostrophic velocity at Point Sur and Point Conception, it seems unlikely that they could account for all of the differences. There are significant differences in the seasonal flow at the two locations computed by any method. The seasonal cycles computed from all available dynamic height data are probably the most reliable estimate of the true seasonal variability. These are the seasonal cycles presented in Section 5. The close agreement between the flow at 150 m and the local poleward pressure gradient at both locations (see section 6) reinforces the credibility of the seasonal cycles computed in this manner.

Acknowledgments. I would like to acknowledge J. McCreary for his very thoughtful comments which greatly improved the manuscript (especially section 3). I would also like to thank J. Reid and B. Hickey for thorough and constructive reviews of the manuscript. K. Brink, C. Mooers, G. Philander, and A. Willmott provided additional very helpful comments. Finally, I would like to thank Anita Lacroix for assistance in typing the manuscript. This work was supported by NASA under contract NAS7-100.

REFERENCES

Allen, J. S., Models of wind-driven currents on the continental shelf, *Ann. Rev. Fluid Mech., 12*, 389–433, 1980.

Bakun, A., and C. S. Nelson, Climatology of upwelling related processes off Baja California, *Calif. Coop. Oceanic Fish. Invest. Rep., 19*, 107–127, 1977.

California Cooperative Oceanic Fisheries Investigations, CalCOFI atlas of 10-meter temperatures and salinities 1949 through 1959, *Atlas*, vol. 1, La Jolla, Calif., 1963.

Cane, M. A., and E. S. Sarachik, Forced baroclinic ocean motions, II, The linear equatorial bounded case, *J. Mar. Res., 35*, 395–432, 1977.

Chelton, D. B., Low frequency sea level variability along the west coast of North America, Ph.D. dissertation, Scripps Inst. of Oceanogr., La Jolla, Calif., 1980.

Chelton, D. B., Statistical reliability and the seasonal cycle: Comments on "Bottom pressure measurements across the Antarctic Circumpolar Current and their relation to the wind," *Deep Sea Res., 29*, 1381–1388, 1982.

Clarke, A. J., Observational and numerical evidence for wind-forced coastal trapped long waves, *J. Phys. Oceanogr., 7*, 231–247, 1977.

Collins, C. A., C. N. K. Mooers, M. R. Stevenson, R. L. Smith, and J. G. Pattulo, Direct current measurements in the frontal zone of a coastal upwelling region, *J. Oceanogr. Soc. J., 24*, 31–42, 1968.

Eber, L. E., Contoured depth-time charts (0 to 200 m, 1950 to 1966) of temperature, salinity, oxygen and sigma-t at 23 CalCOFI stations in the California Current, *Atlas*, vol. 25, California Cooperative Oceanic Fisheries Investigations, La Jolla, Calif., 1977.

Hickey, B. M., The California Current System—hypotheses and facts, *Progr. Oceanogr., 8*, 191–279, 1979.

Hickey, B. M., and N. E. Pola, The seasonal alongshore pressure gradient on the west coast of the United States, *J. Geophys. Res., 88*, 7623–7633, 1983.

Huyer, A., The offshore structure and subsurface expression of sea level off Peru, 1976–1977, *J. Phys. Oceanogr., 10*, 1755–1768, 1980.

Huyer, A., R. L. Smith, and R. D. Pillsbury, Observations in a coastal upwelling region during a period of variable winds (Oregon coast, July 1972), *Tethys, 6*, 391–404, 1974.

Huyer, A., R. D. Pillsbury, and R. L. Smith, Seasonal variation of the alongshore velocity field over the continental shelf off Oregon, *Limnol. Oceanogr., 20*, 90–95, 1975.

Huthnance, J. M., On coastal trapped waves: Analysis and numerical calculation by inverse iteration, *J. Phys. Oceanogr., 8*, 74–92, 1978.

Kundu, P. K., J. S. Allen, and R. L. Smith, Modal decomposition of the velocity field near the Oregon coast, *J. Phys. Oceanogr., 5*, 683–704, 1975.

Lynn, R. J., Seasonal variation of temperature and salinity at 10 m in the California Current, *Calif. Coop. Oceanic Fish. Invest. Rep., 19*, 157–174, 1967.

Lynn, R. J., K. A. Bliss, and L. E. Eber, Vertical and horizontal distributions of seasonal mean temperature, salinity, sigma-t, stability, dynamic height, oxygen, and oxygen saturation in the California Current, 1950–1978, *Atlas*, vol. 30, California Cooperative Oceanic Fisheries Investigations, La Jolla, Calif., 1982.

McCreary, J. P., Eastern tropical ocean response to changing wind systems: With application to El Niño, *J. Phys. Oceanogr., 6*, 632–645, 1976.

McCreary, J. P., Eastern ocean response to changing wind systems, Ph.D. dissertation, Scripps Inst. of Oceanogr., La Jolla, Calif., 1977.

McCreary, J. P., A linear stratified model of the coastal undercurrent, *Phil. Trans. R. Soc. London, 302*, 385–413, 1981.

Mooers, C. N. K., C. A. Collins, and R. L. Smith, The dynamic structure of the frontal zone in the coastal upwelling region off Oregon, *J. Phys. Oceanogr., 6*, 3–21, 1976.

Nelson, C. S., Wind stress and wind stress curl over the California Current, *Tech. Rep. NMFS-SSRF-714*, Nat. Oceanic and Atmos. Admin., Washington, D.C., 1977.

O'Brien, J. J., R. M. Clancy, A. J. Clarke, M. Crepon, R. Ellsburg, T. Grammelsrod, M. MacVean, L. P. Reed, and J. D. Thompson, Upwelling in the Ocean: Two- and three-dimensional models of upper ocean dynamics and variability, in *Modelling and Prediction of the Upper Layers of the Ocean*, edited by E. B. Kraus, pp. 178–228, Pergamon, New York, 1977.

Pedlosky, J., Longshore currents, upwelling and bottom topography, *J. Phys. Oceanogr., 4*, 214–226, 1974.

Philander, S. G. H., and J. H. Yoon, Eastern boundary currents and coastal upwelling, *J. Phys. Oceanogr., 12*, 862–879, 1982.

Reid, J. L., Measurements of the California Countercurrent at a depth of 200 m, *J. Mar. Res., 20*, 134–137, 1962.

Reid, J. L., Measurements of the California Countercurrent off Baja California, *J. Geophys. Res., 68*, 4819–4822, 1963.

Reid, J. L., and A. W. Mantyla, The effect of the geostrophic flow upon coastal sea level variations in the northern Pacific Ocean, *J. Geophys. Res., 81*, 3100–3110, 1976.

Reid, J. L., and R. A. Schwartzlose, Direct measurements of the Davidson Current off central California, *J. Geophys. Res., 67*, 2591–2597, 1962.

Reid, J. L., G. I. Roden, and J. G. Wyllie, Studies of the California Current system, *Calif. Coop. Oceanic Fish. Invest. Rep., 5*, 28–57, 1958.

Reid, J. L., R. S. Schwartzlose, and D. Brown, Direct measurements of a small surface eddy off northern Baja California, *J. Mar. Res., 67*, 2491–2497, 1963.

Sverdrup, H. U., and R. H. Fleming, The waters off the coast of southern California, March to July 1937, *Scripps Inst. Oceanogr. Bull., 4*, 261–387, 1941.

Sverdrup, H. U., M. W. Johnson, and R. H. Fleming, *The Oceans: Their Physics, Chemistry and General Biology*, Prentice-Hall, Englewood Cliffs, N.J., 1942.

Tsuchiya, M., Inshore circulation in the Southern California Bight, 1974–1977, *Deep Sea Res., 27A*, 99–118, 1980.

Wang, D. P., and C. N. K. Mooers, Coastal trapped waves in a continuously stratified ocean, *J. Phys. Oceanogr., 6*, 853–863, 1976.

Wooster, W. S., and J. H. Jones, California undercurrent off northern Baja California, *J. Mar. Res., 28*, 235–250, 1970.

Wooster, W. S., and J. L. Reid, Eastern boundary currents, in *The Sea*, vol. 6, edited by M. N. Hill, pp. 253–260, Wiley-Interscience, New York, 1963.

Wyllie, J. G., Geostrophic flow of the California Current at the surface and at 200 m, *Atlas*, vol. 4, California Cooperative Oceanic Fisheries Investigations, La Jolla, Calif., 1966.

Wyllie, J. G., and R. J. Lynn, Distribution of temperature and salinity at 10 m, 1960–1969, and mean temperature, salinity and oxygen at 150 m, 1950–1968, in the California Current, *Atlas*, vol. 15, California Cooperative Oceanic Fisheries Investigations, La Jolla, Calif., 1971.

D. B. Chelton, College of Oceanography, Oregon State University, Corvallis, OR 97331.

(Received September 9, 1983;
revised January 19, 1984;
accepted January 20, 1984.)